Estimation of Breast Tumor Location using Phase Information and Received Signal Delay

Mohammad Ali Pourmina, Javad Nouripour, Mohamad Naser Moghaddasi, Behbod Ghalamkari
Faculty of Mechanical, Electrical and Computer Engineering, Science and Research Branch, Islamic Azad University, Tehran, Iran.
Email: pourmina@srbiau.ac.ir

Received: January 2022 Revised: March 2022 Accepted: April 2022

ABSTRACT:
In this article, a new method is proposed to find tumor's location. This process is based on the arrangement of sensors; the phase and distance to the cancer are given as well. Extraction of tumor distance and phase by Snell's law is the number of received pulses and the delay of receiving Signal. The transmitter antenna is in a fixed position, and the receiver rotates at a certain angular velocity around the tissue. Considering this information, a package solution in polar coordinates is presented. Meanwhile, angle and range information are extracted. Then the maximum probability estimate of the target location is given. This paper applies experimentally to simulated random data.

Keywords: Tumor, interferometry, maximal probability, time difference of reception, breast tissue

1. INTRODUCTION

Diagnosis of breast tumors has always been difficult by the means of radio because the reflex reasons for the cancer include two types of early and late time signals. When signals are early reflected from the skin, they are the ones who signal the response of the tumor and the clitoris. Preprocessing algorithms eliminate the early scatter field time indicator [1]. Identification methods for tumor detection or clitoris removal are presented in this paper [1]. It also represents a method for estimating tumor response in scattered fields. This method uses a technique to model the temporal response. The Inductive Maximum Estimation Scheme (MAP) has been applied to evaluate the exchange rate for the currencies used [1].

Accurate detection of the tumor response allows the clutter to be isolated from the late reply.

This paper presents a method for estimating the tumor response in late scattered fields. This method uses a function to model the tumor response.

Determination of maximum inductive estimation has been applied for optimal evaluation of estimates. Pattern classification methods are then used. In this article [3], we review recent research in this field. First, we introduce the concept of microwave imaging through the formation of space-time beam (MIST) and related decision algorithms. The purpose of these processing techniques is to create a spatial image of scattered microwave energy and to identify the location of malignant lesions as signs of their scattering as well.

Then, studies of time-domain simulations offer finite differences to demonstrate the effect of MIST radiation formation on the diagnosis of small malignant breast tumors in both susceptible and passive structures. In addition, adaptive radar tumor detection of a tissue sensor has been suggested for the early detection of breast cancer. Tumor diagnosis is employed using differences in the electromagnetic properties of malignant tumors and surrounding healthy breast tissue (fat). Scattered fields are recorded and processed to amplify the tumor response. Then different algorithms are used for analysis. Various applications are applied to the processed programs from antenna positions which make it possible to detect and determine the location of tumors. In this article, first, the geometry of the cancer is described to locate the tumor. In the radar section, the cancer is discussed. In the areas after the radar stage, the cancer is considered. And we present the solution of the package in terms of angle and time difference. Moreover, the probability estimation information (MLE) is said, its simulated events are applied and reported.

2. PROBLEM GEOMETRY

The problem is shown in Figure 1 Geometry. In this figure, we see that the transmitter is in a particular position where there is a (tumor) in an unknown place, i.e. its location is not known. In order to find the place of the cancer, a moving node rotates around it. The return signal from the cancer has specific changes, and

Paper type: Research paper
DOI: https://doi.org/10.30486/mjtd.2022.695916
How to cite this paper: M. A. Pourmina, J. Nouripour, M. N. Moghaddasi and B. Ghalamkari, "**Estimation of Breast Tumor Location using Phase Information and Received Signal Delay**", Majlesi Journal of Telecommunication Devices, Vol. 11, No. 2, pp. 61-66, 2022.

the moving node rotates around the breast tissue at a certain angular velocity. It receives the return signal from the cancer, assuming the angle of the transmitter node. The moving node calculates the amount of signal deviation from the straight line.

At any given moment, we extract the input phase according to the number of transmitted waves and to the angular velocity of ninety. To calculate the range, we calculate the amount of deviation.

Fig. 1. Tumor-free radiation b Tumor-free radiation.

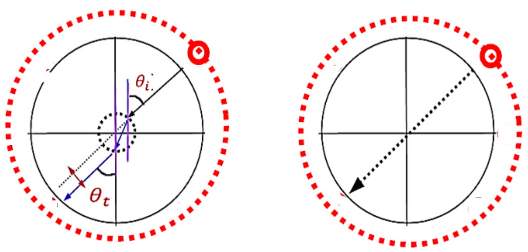

Solve the tumor location package to obtain the position of the tumor from zinc, and there is an angle and a difference. First, the radar cross-section of the tumor is extracted, then the angle and range are extracted according to Snell's law and the number of received waves. As shown in Figure 1, if the target radar cross-section is not detected, the transmitted frequency is changed so that at a particular frequency, the tumor resonates and reflects the signal. Therefore, the frequency [4] is set and the target is at the resonant frequency. Accordingly, the radar signal can be returned. As a result, the received frequency and wavelength are obtained, and then a circle with a wavelength radius of $\lambda \cong r$ is drawn in the chest. Whether this is a cancerous tumor or not is determined, but its direction and location are unknown [5]. (So, the cross-sectional area of the target radar is equal to the resonance area.)

$\sigma = 4\pi r^2 \quad imum\ point;$
$\sigma = 0.26\pi r^2 \quad imum\ point$

By changing the wave's frequency as it passes through the tumor, it fails. The propagation path of the wave changes, so the information we obtained is the position of the cancer in terms of angle and angular difference. As mentioned above, the signal reception angle is achieved according to the speed of the moving node angle and the time difference according to Snell's law and the number of received waves.

At each rotation, we know the radiation angle, so the angle of reflection is calculated relative to the time when the light is refracted if we do not have light refraction.

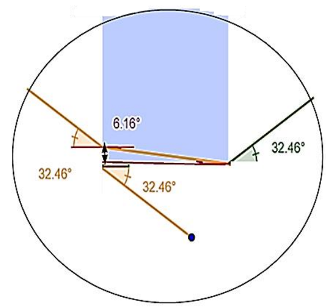

Fig. 2. Shows the angle of refraction and its effect on the charity of time.

$$\boldsymbol{r_{diff} = r_i - r_1; \Rightarrow \lambda \approx r} \tag{1}$$

In Equation 2, light refraction causes the wave propagation velocity to decrease. This wave velocity reduction is defined according to the tumor permeability coefficient. According to Table 1, the permittivity of tumor tissue is $\frac{n_2}{n_1}$ equal to the environment. Using the Snell relation and changing the frequency, if the wavelength is less than the cross-sectional area of the target radar, it causes the wave to pass.

$$\boldsymbol{n = \frac{c}{v} \Longrightarrow v = \frac{c_0}{\sqrt{\varepsilon_r}}} \tag{2}$$

$$\boldsymbol{\sin\theta_2 = \frac{n_1}{n_2}\sin\theta_1; \Rightarrow \sin\theta_3 = \frac{n_2}{n_1}\sin\theta_2;} \tag{3}$$

In the above equation, the v velocity of the wave propagation in the medium is n_1, n_2 the refractive index of the two media, $sin\theta_1$ the wave entry angle, and $\sin\theta_2$ the wave exit angle.

Table 1. Profile of breast tissue.

Type of texture	Dielectric coefficient $\sigma\left[\frac{S}{m}\right]$	Transmission coefficient ε_r
Skin	4	36
Tumor	4	50
Breast	0.44-0.36	9.9-8.1

2.1. Phase Extraction

Phase difference measurement between different places, where the node moves are used to calculate the angle of the input signal, is available. By measuring the phase difference (interference) between other locations, the angle of the input signal in different directions can be obtained. This method is computationally complex, which can be achieved by changing the computational pattern to select specific scenarios instead of using all of them.

$$\theta_i = sin^{-1}\left(\frac{\lambda(2k\pi + d\varphi)}{2\pi\ dr\ tan\theta_j}\right)$$

Where dr the distance between two different locations is, λ is the wavelength of the received signal, θ is the angle of the received signal, and $d\varphi$ is the phase difference calculated between the two antennas.

The main challenge in this formula arises when λ has small values; When the $\frac{\mathrm{d}}{\lambda}$ ratio is greater than $\frac{1}{2}$, the phase detection ambiguity is created. According to the phase calculation formula, when λ has small values, $d\varphi$ can contain different coefficients of $2k\pi$. That is, all values for which the value opposite the sine formula is less than one will be part of the answer set.

In this case, it should be considered for more than one distance to remove the ambiguity. It is worth mentioning that these distances should be different [6].

2.2. Extract the Board based on a Time Difference

The TDOA-based algorithm uses the difference in propagation time from the source to the receptors due to the relative permeability drop [7]. This section briefly proposes this TDOA-based algorithm. The lower relative permeability of the tumor area reduces the time delay from origin to the recipient. This difference in time delay works as follows. Suppose τ_0 and τ_n are times when signals are received at different times in different places. Where τ^{AB} denotes the transition times from n_A (position) to n_B. Defines $\in_n$ as the dielectric constant of the tissue within the tumor region at the nth moment and defines $\in_0$ as the dielectric constant of the tissue from other areas. TDOAs are approximated in different places according to the following relation:

$$\boldsymbol{\Delta\tau = \tau_0 - \tau_n \cong \left(1 - \sqrt{\xi}\right)\tau_0\ ;\ \xi = \frac{\in_n}{\in_0}} \quad (2)$$

Due to the delay in receiving the pulse, we find the distance of the tumor from the skin.

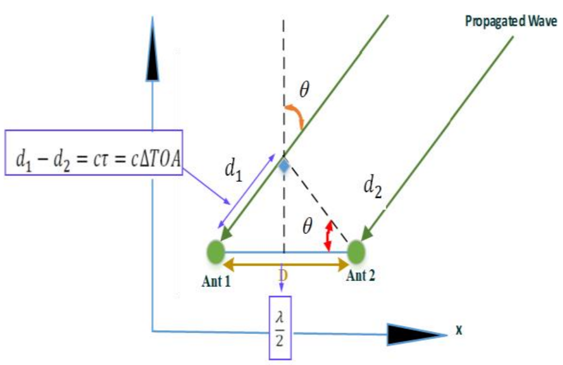

Fig. 3. Calculating the time difference of receiving in different places.

$$\boldsymbol{dr = d_1 - d_2 = c\tau = c\Delta TOA = \Delta d = \frac{\lambda}{2} = L = 2\pi r\frac{\theta Angle\ deviation}{180^0}} \quad (3)$$

$$\boldsymbol{d\varphi = \frac{2\pi dr}{\lambda}sin\theta \Rightarrow dr = \frac{d\varphi\lambda}{2\pi sin\theta}} \quad (6)$$

We introduce a wave time difference algorithm in which the frequency dependence in the propagation medium is compensated for by considering the conductivity drop in the evaluation. This decrease in conductivity affects not only the amplitude of the scattered front of the signal, but also the phase of the signal. Waveform reconstruction to retrieve this phase information can further improve accuracy and precision.

As in Fig. 4, we solve the equations using the TDOA algorithm. Also, the phase difference of the received signal in a closed-form in polar coordinates and the results are in the form of Equation 8.

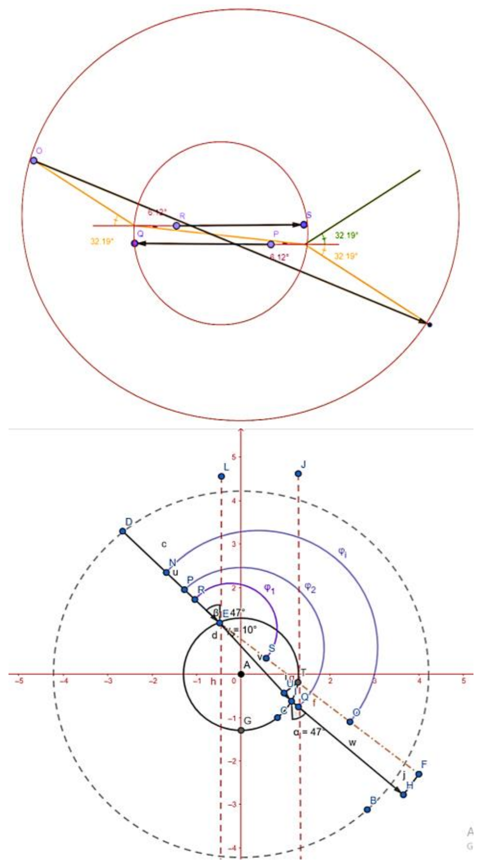

Fig. 4. General geometry of the problem.

$$\begin{cases} R_i = k(\omega)\frac{(dr+1)}{\mathrm{d}\varphi} \\ \theta_i = sin^{-1}\left(\frac{\lambda(2k\pi+d\varphi)}{2\pi\ dr\ tan\theta_j}\right) \xrightarrow{dr=d\acute{r}\ tan\theta_j} \theta_i = sin^{-1}\left(\frac{\lambda(2k\pi+d\varphi)}{2\pi\ dr}\right) \end{cases} \quad (7)$$

2.3. Estimating the Maximum Probability

Suppose we have several observations for one cancer. Because the return signal from the cancer is rippled in the direction of vision $\sigma(\theta,\varphi)$, the locations obtained for a tumor from each observation will not be the same. As mentioned above, the viewing angle is achieved by the sensor, and the signal reception is delayed.

If these two parameters have noise with Gaussian distribution, we assume that the time difference noise is also Gaussian. So we have:

$$\begin{cases} \mathbf{dr} = \mathbf{dr_0} + \mathbf{n_{dr_0}}, & \mathbf{n_{R_{dif}}} \sim \boldsymbol{\mathcal{N}}(\mathbf{0}, \boldsymbol{\sigma}^2_{\mathbf{R_{dif}}}) \\ \quad \mathbf{d\varphi} = \mathbf{d\varphi_0} + \mathbf{n_{d\varphi}}, & \mathbf{n_{d\varphi}} \sim \boldsymbol{\mathcal{C}}(\mathbf{0}, \boldsymbol{\sigma}_{\mathbf{d\varphi}}) \end{cases} \tag{8}$$

In this relation, dr_0 is the value of the longitudinal difference which is added by Gaussian mass noise $n_{dr_0}$with zero mean and variance $\sigma^2_{dr_0}$ and $d\varphi_0$ is the value of the angle with Group noise $n_\theta$is summed with Gaussian mass noise with parameters zero and dr. We also consider angle noise independent of temporal difference noise.

$$\boldsymbol{f_{dr d\varphi}(dr, d\varphi) = f_{dr}(dr) f_{d\varphi}(d\varphi) =} \\ \frac{\mathbf{1}}{\boldsymbol{\sigma_{dr}\sqrt{2\pi}}} \boldsymbol{e}^{\frac{(\boldsymbol{dr-dr_0})^2}{\boldsymbol{2\sigma^2_{dr}}}} \frac{\mathbf{1}}{\boldsymbol{\sigma_{d\varphi}\sqrt{2\pi}}} \boldsymbol{e}^{\frac{(\boldsymbol{d\varphi_0-d\varphi})^2}{\boldsymbol{2\sigma^2_{d\varphi}}}} \tag{9}$$

In this relation, $f_{d\varphi}(d\varphi)$ is the probability distribution function $d\varphi$ and $f_{dr}(dr)$ is the probability distribution function dr and $f_{drd\varphi}(dr, d\varphi)$ is the common distribution function $d\varphi$ and dr . We have this distribution function for every time difference and angle. Now we want to get the function of the typical distribution function of the distance R_i and the angle θ_i from this relation. To do this, we must solve Equations (11) in terms of R_i and θ_i. Given the geometry of the problem, we have a special dr and $d\varphi$ for R_i andθ_i, so we will arrive at a single answer. Using Figure 4 and simplification, dr and $d\varphi$ in terms of R_i and θ_i as follows:

$$\begin{cases} R_i = k(\omega)\dfrac{(dr+1)}{d\varphi} = \dfrac{k(\omega)dr + k(\omega)}{d\varphi} \Rightarrow dr = \dfrac{R_i d\varphi - k(\omega)}{k(\omega)} \\ \Rightarrow dr \\ d(\varphi_i - \varphi_{i-1}) = \dfrac{2\pi D \sin\theta_i - 2k\lambda\pi}{\lambda} \end{cases} \tag{10}$$

The standard probability distribution function of distance and angle$f_{R_i\theta_i}(R_i,\theta_i)$ from $f_{drd\varphi}(dr, d\varphi)$ can be obtained as follows:

$$\boldsymbol{f_{R_i\theta_i}(R_i,\theta_i) = \frac{f_{drd\varphi}(dr,d\varphi)}{|J(dr,d\varphi)|}} \tag{4}$$

(12) The Jacobin matrix $\left(J(R_i,\theta)\right)$ is as follows:

$$|J(d\varphi, dr)| = \begin{bmatrix} \dfrac{\partial R_i}{\partial d\varphi} & \dfrac{\partial R_i}{\partial dr} \\ \dfrac{\partial \theta_i}{\partial d\varphi} & \dfrac{\partial \theta_i}{\partial dr} \end{bmatrix} \\ = \begin{bmatrix} \dfrac{k(\omega)dr + k(\omega)}{(d\varphi)^2} & \dfrac{k(\omega)}{(d\varphi)^2} \\ \dfrac{\lambda\, dr}{2\pi(\,dr)^2} & \dfrac{\lambda(2k\pi + d\varphi)}{2\pi\,(dr)^2} \end{bmatrix} \\ \Rightarrow \; |J(d\varphi, dr)| \\ = \left| \left(\frac{(k(\omega)dr + k(\omega))(2k\pi\lambda + \lambda d\varphi)}{(d\varphi)^2 2\pi\,(dr)^2} \right) \right. \\ \left. - \left(\frac{k(\omega)\lambda\, dr}{(d\varphi)^2 2\pi(\,dr)^2} \right) \right| \\ = \left| \left(\frac{k(\omega)\lambda^2 dr d\varphi + k(\omega)\lambda^2 d\varphi - k(\omega)\lambda\, dr}{d\varphi^2 dr^2} \right) \right| \tag{12}$$

Finally, for the common distribution function, we have R_i andθ_i:

$$f_{R_i\theta_i}(R_i,\theta_i) \\ = \frac{1}{\sigma_{dr}\sqrt{2\pi}} e^{\frac{(dr-dr_0)^2}{2\sigma^2_{dr}}} \frac{1}{\sigma_{d\varphi}\sqrt{2\pi}} e^{\frac{(d\varphi_0-d\varphi)^2}{2\sigma^2_{d\varphi}}} \\ * abs\left(\frac{k(\omega)\lambda^2 dr d\varphi + k(\omega)\lambda^2 d\varphi - k(\omega)\lambda\, dr}{d\varphi^2 dr^2} \right) |_{r_d = k(R_i,\theta_i),\theta_i d\varphi = z(R_i,\theta_i)} \tag{13}$$

In this regard, the operator's $abs(.)$ represents the absolute value. If the observation information of one containing rd and $d\varphi$ is known, the probability distribution function $R_i$and $\theta_i$is fully specified. If we have N observations for one and the noises are independent of each other, the probability distribution function concerning all observations is as follows:

$$\begin{cases} f_{R_i\theta_i}(R_i,\theta_i|Observation) = \prod_{k=1}^{N} f_{R_i\theta_i|Obs_k}(R_i,\theta_i|Observation_k) \\ All\ Obs = \{Observation_k\} \quad k = 1, \ldots, N \end{cases} \tag{14}$$

The Maximum Probability Estimator (MLE) is as follows:

$$(R_i,\theta_i)_{ML} = \underset{R_i,\theta_i}{\operatorname{argmax}}\left(\prod_{k=1}^{N} f_{R_i\,\theta_i}(R_i,\theta_i|Observation_k)\right)$$
$$= \underset{R_i,\theta_i}{\operatorname{argmax}}\left(\sum_{k=1}^{N} \ln f_{R_i\,\theta_i}(R_i,\theta_i|Observation_k)\right) \quad (15)$$

The coordinates $(R_i,\theta_i)_{ML}$give us the most likely location. Finding the maximum of this function directly by solving it is very complicated due to its nonlinearity.

3. SIMULATION AND EVALUATION

Tumor assessors are used for data collected from different antenna positions. At each antenna position, the received signal has a time delay and an angle that indicates the random location of the tumor. (Due to the rotation of the antenna around the tissue, in some situations the antenna is farther from the tumor, and in some cases, the antenna is closer to the tumor).

In this section, the performance of the estimation method is evaluated. It is noteworthy that the results are also compared with the Rao Kramer band.

1. The tumor is in the direction of the x-axis and is measured every 2 mm for a range of 15 cm of target data.
2. The standard deviation of the angle measurement error is considered to be 0.2 degrees.
3. Assuming the target is at distances of 40, 30, 20 cm. Using The Rao Kramer low band and the Monte Carlo method, the standard deviation of the range and angle can be easily calculated; Figures 6 and 7 show this comparison.

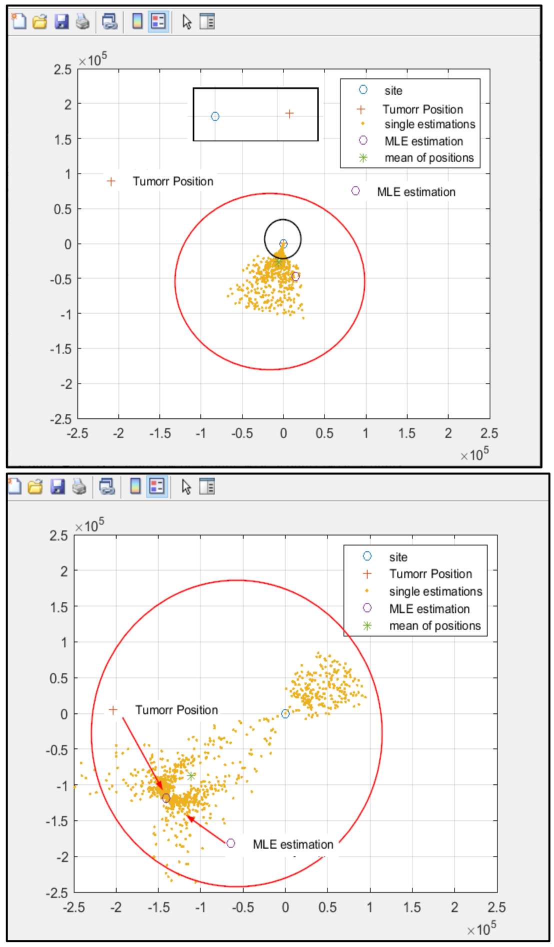

Fig. 5. Round view Estimating the target location using the maximum likelihood method.

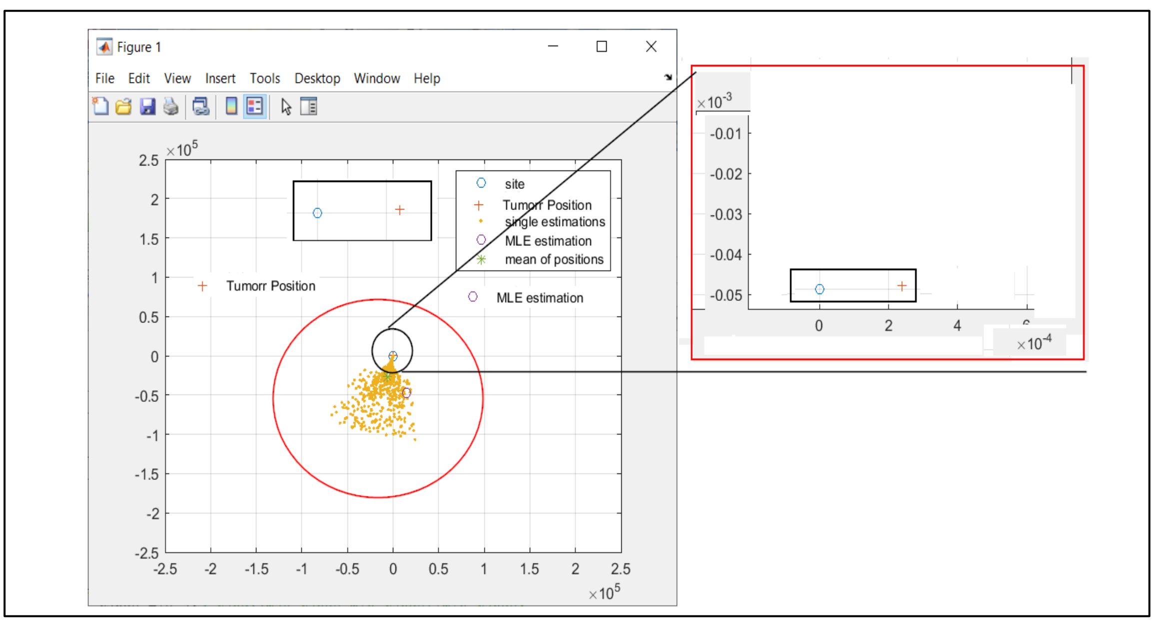

Fig. 6. Close view of target location estimation using the maximum likelihood method.

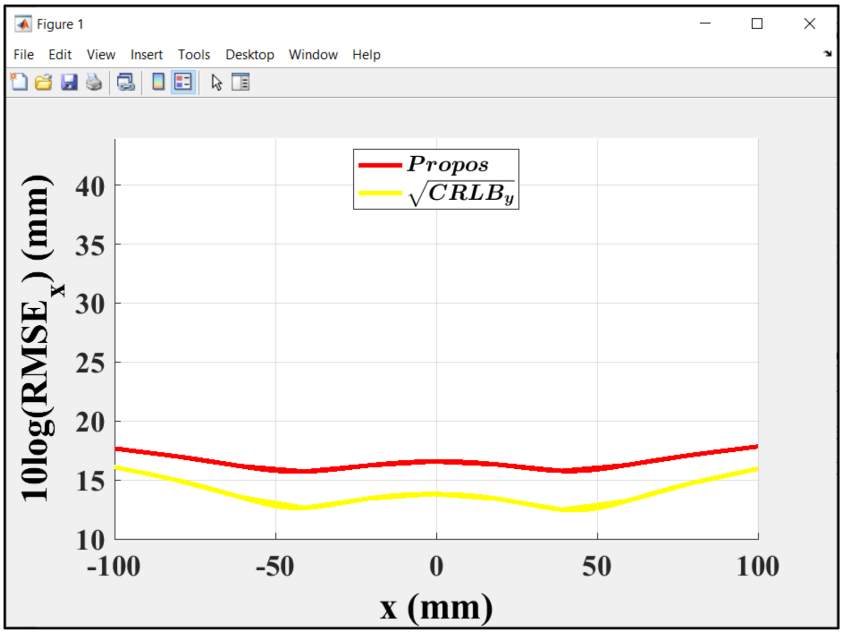

Fig. 7. Comparison of the proposed method with The Rao Kramer band.

We now compare the estimated positions with the exact location of the tumor. The estimated place through the ML is about 2 mm from the precise position, and given that the cancer is about 20 cm from the recipient, we have an error of about 2%.

4. CONCLUSION

This article seeks to provide an optimal method for locating the donor tumor. The transmitter antenna is in a fixed position and the receiver rotates at a certain angular velocity around the tissue. With any MLE method, the problem can be solved. In this paper, the tumor's location was found using a node, and using this information, a package solution in polar coordinates is presented, angle and range information is extracted. Then the maximum probability estimate of the target location is given.

REFERENCES

[1] D. J. Kurrant, E. C. Fear and D. T. Westwick, **"Tumor Estimation In Tissue Sensing Adaptive Radar (TSAR) Signals,"** *in 2007 Canadian Conference on Electrical and Computer Engineering, Vancouver*, BC, Canada, pp. 22-26 April 2007.

[2] F. M. a. D. T. W. Douglas J. Kurrant, **"Tumor Response Estimation in Radar-Based Microwave Breast Cancer Detection,"** *IEEE Transactions On Biomedical Engineering*, Vol. 55, p. 12, DECEMBER 2008.

[3] K. Kanazawa, K. Noritake, Y. Takaishi, and S. Kidera, **"Microwave Imaging Algorithm Based on Waveform Reconstruction for Microwave Ablation Treatment,"** *IEEE Transactions on Antennas and Propagation*, pp. Volume: 68, Issue: 7, July 2020.

[4] B. S. Javad. Nooripor, **"Disorder system signal spectrum to steal Velocity Range Gate,"** *Majlesi Journal of Telecommunication Devices*, Vol. 2, No. 2322-1550, p. 2, June 2012.

[5] G. W. STIMSON, Introduction AIRBORNE Radar, MENDHAM, NEW JERSEY: SciTech Publishing, 1983.

[6] S. V. Doan, J. Vesely, P. Janu, P. Hubacek, and X. L. Tran, **"Optimized algorithm for solving phase interferometer ambiguity,"** *in 2016 17th International Radar Symposium (IRS)*, Krakow, Poland, 10-12 May 2016.

[7] K. Kanazawa, K. Noritake, and Y. T. a. S. Kidera, **"Microwave Imaging Algorithm Based on Waveform Reconstruction for Microwave Ablation Treatment,"** *IEEE Transactions on Antennas and Propagation*, Vol. 68, No. 7, pp. 5613 - 5625, 2020.